Cellular Immunology 397-398 (2024) 104814

Contents lists available at ScienceDirect

Cellular Immunology

journal homepage: www.elsevier.com/locate/ycimm

Research paper

MALT1 inhibition suppresses antigen-specific T cell responses

Iliana K. Kerzeli [a], Aikaterini Nasi [a], Erika Fletcher [a], Aikaterini Chourlia [a], Anders Kallin [b], Niklas Finnberg [b], Karolina Ersmark [b], Maria Lampinen [a], Mark Albertella [b], Fredrik Öberg [b], Sara M. Mangsbo [a,*]

[a] Department of Pharmacy, Science for Life Laboratory, Uppsala University, Uppsala, Sweden
[b] Medivir AB, Lunastigen 5, 141 22 Huddinge, Sweden

ARTICLE INFO

Keywords:
MALT1 inhibition
T regulatory cells
T-cell dependent immune surveillance

ABSTRACT

The aim of this study was to assess the potential use of a selective small molecule MALT1 inhibitor in solid tumor treatment as an immunotherapy targeting regulatory *T*-cells (Tregs). In vitro, MALT1 inhibition suppressed the proteolytic cleavage of the MALT1-substrate HOIL1 and blocked IL-2 secretion in Jurkat cells. It selectively suppressed the proliferation of PBMC-derived Tregs, with no effect on conventional $CD4^+$ *T*-cells. In vivo, however, no evident anti-tumor effect was achieved by MALT1 inhibition monotherapy or in combination with anti-CTLA4 in the MB49 cancer model. Despite decreased Treg-frequencies in lymph nodes of tumor-bearing animals, intratumoral Treg depletion was not observed. We also showed that MALT1-inhibition caused a reduction of antigen-specific $CD8^+$ *T*-cells in an adoptive *T*-cell transfer model. Thus, selective targeting of Tregs would be required to improve the immunotherapeutic effect of MALT1-inhibition. Also, various dosing schedules and combination therapy strategies should be carefully designed and evaluated further.

1. Introduction

Regulatory *T*-cells (Tregs) are a specialized subpopulation of *T*-cells characterized by the expression of the transcription factor FoxP3. These cells are essential for maintaining peripheral tolerance, preventing autoimmune disease and limiting chronic inflammatory diseases [1]. However, Tregs also infiltrate into tumor tissues, where they suppress effective tumor immunity and are associated with a poor prognosis [2]. Strategies to limit the immune suppressive effect of Tregs in cancer without eliciting autoimmunity are therefore warranted.

One of the emerging strategies is to target the activity of mucosa-associated lymphoid tissue lymphoma translocation 1 (MALT1). The MALT1 protein was initially identified as a key driver in MALT lymphomas and in diffuse large B cell lymphoma, making it an attractive target for lymphoma therapy [3–6]. This arginine-specific paracaspase is part of the CARD11–BCL10–MALT1 (CBM) complex, which regulates NF-κB activation downstream of cell surface receptors [7,8], and as such is an important factor in T- and B-cell homeostasis [9–14]. Moreover, MALT1 possesses the capacity of autocleavage, which is an additional necessary step in NF-κB activation [15,16]. Apart from BCL10 cleavage and its auto-cleavage, MALT1 proteolytically cleaves the signaling regulators A20 [17], CYLD [18], HOIL-1 [19–21], and the NF-κB family member RelB [22]. CBM-signaling, in a MALT1-dependent manner, has been shown to mediate the conversion of resting Tregs to effector Tregs by inducing NF-κB activation [23,24]. This finding has opened up the possibility for using MALT1-inhibition as a way of reducing Tregs in the tumor microenvironment.

Indeed, inactivation of the CBM complex and specifically MALT1-inhibition could enhance antitumor immune responses and prime tumors for immune checkpoint therapy, as demonstrated in several murine tumor models combining MALT1 inhibitor with anti- programmed cell death protein 1 (PD1) [25–27]. This priming effect is mainly due to the ability of MALT1-inhibition to convert Tregs into IFN-γ-producing effector cells. However, the combination of MALT1-inhibition with CTLA-4 blockade is less investigated, and thus there is a lack of understanding of potential pitfalls in using immune checkpoint therapies that rely on de novo T cell generation for anti-tumor efficacy.

In a study on $Foxp3^{Cre}Malt1^{fl/C472A}$ mice, in which Malt1 protease

Abbreviations: MALT1, mucosa-associated lymphoid tissue lymphoma translocation1; Treg, regulatory *T*-cell; PBMC, peripheral blood mononuclear cell; CTLA4, cytotoxic *T*-lymphocyte associated protein4; CBM complex, CARD11-BCL10-MALT1 complex; NK-cells, natural killer cells, DCs, conventional dendritic cells; MDSCs, monocytic derived suppressor cells; IP, intraperitoneal; SC, subcutaneous.

* Corresponding author.
E-mail address: sara.mangsbo@farmaci.uu.se (S.M. Mangsbo).

https://doi.org/10.1016/j.cellimm.2024.104814
Received 3 January 2024; Received in revised form 22 February 2024; Accepted 23 February 2024
Available online 24 February 2024
0008-8749/© 2024 The Authors. Published by Elsevier Inc. This is an open access article under the CC BY license (http://creativecommons.org/licenses/by/4.0/).

was specifically inactivated in Treg cells, the mice developed spontaneous inflammatory disorders, but loss of MALT1 autocleavage capacity also led to reduction of tumor growth [25,28].

A plethora of small molecule MALT1 inhibitors targeting its proteolytic activity have been examined in vitro and in vivo for potential use in lymphomas. Among those MI-2, a covalent and non-reversible suicide inhibitor acting on the catalytic center of MALT1 [29,30], the peptide-based compound VRPR-fmk [7], and pyrazolopyrimidine derivatives [31] have been developed and preclinically proven efficient with lymphoma cell lines or animal models of hematological malignancies.

There are a number of ongoing clinical trials of MALT1 inhibitors, of which the first was initiated in 2019 as a phase 1, first-in-human, open-label study of safety, pharmacokinetics and pharmacodynamics in patients with Non-Hodgkin's Lymphoma and Chronic Lymphocytic Leukemia (ClinicalTrials.gov Identifier: NCT03900598).

The aim of this study was to assess the potential impact of selectively inhibiting MALT1 in solid tumor treatment using a mouse model of urothelial cancer. We performed pharmacokinetic characterization of the inhibitor and evaluated its effects on *T*-cells in vitro and in vivo along with anti-tumor effects as monotherapy and in combination with anti-CTLA-4 therapy.

2. Materials and methods

2.1. MALT1 inhibitor compound

The inhibitor of MALT1, herein named MV088428, was synthesized as described in Pissot Soldermann, C. et al 2015 WO2015/181747 (also described by Quancard *et al* as MLT-985 [32]) and formulated for either in vitro or in vivo use (administration per os (PO)).

2.2. MALT1 enzyme assay

Full-length MALT1 enzyme at 2 nM was assayed in 50 mM HEPES, 100 mM NaCl, 0.9 M NaCitrate, 1 mM EDTA, pH 7.5, with 50 μM Ac-Leu-Arg-Ser-Arg-AMC as substrate. Compound was added in an 11-point concentration series from 100 μM to 1 nM in half-log dilution. Compound were distributed in 384 well plates by Echo550, and the assay was run with fluorescence readings at 460 nm, every 2 min for 60 min.

2.3. Western blot

Following activation with PMA/ionomycin 1hr after exposure to 0.1 % DMSO or 3 μM MALT1 inhibitor, whole-cell lysates of Jurkat cells were run with Protein Simple (Peggy Sue, size separation mode) using Size Master kit. A mix of anti-HOIL1 (#sc-393754, Santa Cruz), anti-pIKK (#2078), anti-pIκBα (#4814), pJNK (#4668) and anti-COX IV (#4850, all from Cell Signaling) was used. COX IV was used as a loading control.

2.4. IL-2 expression

Jurkat cells in culture were preincubated with MALT1 inhibitor for 30 min and then stimulated by PMA/Ionomycin for 24 h. IL-2 protein in medium of activated Jurkat cells was measured after 40 h using MesoScale S600 with a human IL-6 tissue culture kit according to manufacturer's recommendations (MSD).

2.5. In vitro differentiation of human Treg cells

Peripheral blood from healthy donors was used for the studies on human cells. Naïve $CD4^+$ *T*-cells were sorted and stimulated for Treg induction. A flat-bottom 48 well plate was coated with functional grade anti-human CD3 at 2 μg/ml in PBS. The plate was sealed and incubated at 37 °C for one hour. Peripheral blood mononuclear cells (PBMCs) were isolated from human leucocyte reduction system cones by differential density centrifugation using Ficoll-PLUS (GE Healthcare). Cells were washed three times and then resuspended at a concentration of $200x10^6$/ml of RPMI + 1 % HI-FCS + 1 % penicillin/streptomycin (P/S) (1 % RPMI). An aliquot of cells was set aside for single color controls, and the sample was stained at a dilution of 1:20 with anti-human CD4, anti-human CD45RA, anti-human CD25, and anti-human CD127 (antibodies from BioLegend and eBioscience) for 20 min on ice. Following the incubation, the stained PBMCs were washed and resuspended at $50x10^6$/ml in PBS + 1 % heat-inactivated fetal calf serum (HI-FCS). Cells were sorted on a BD FACSARIA high speed cell sorter for the phenotype $CD4^+$ $CD45RA^+$ $CD127^+$ $CD25^-$. Following the sort, cells were resuspended at $4x10^6$/ml in pre-warmed complete RPMI (cRPMI) containing 4x 400 U/ml human IL-2 (final concentration 100 U/ml). In each well of the washed anti-CD3-coated 48 well plate, 250 μl of 4x 8.0 μg/ml anti-CD28 (eBioscience) and 250 μl of 4x drug (0.16, 1.6 or 16 μM compound MV088428) were added. Either 250 μl of cRPMI or 250 μl of 4x 4.0 ng/ml TGFβ were added per well, as appropriate. Finally, 250 μl of cells were added per well. The plate was incubated for 5 days at 37 °C with 5 % CO_2. After five days, cells were transferred to polypropylene tubes and washed twice with cRPMI. Cells were then resuspended in IL-2 ± TGFβ with vehicle control or MALT1 inhibitor compound. The plate was incubated for an additional 5 days at 37 °C with 5 % CO_2. On day 10 induced Treg cultures were washed and counted. Aliquots were stained with Fixable Viability Dye eFluor® 780 (eBioscience) then washed and stained for surface expression of CD25. After staining, cells were fixed, permeabilized and stained for intracellular expression of Foxp3 per manufacturer's instructions (Human Foxp3 Buffer set and anti-human Foxp3 antibody from BD Pharmingen). Following staining, cells were washed and resuspended in PBS + 1 % HI-FCS (FACS buffer). Samples were run within four hours on a CyAn™ ADP Analyzer.

2.6. Functional activity assessment of in vitro differentiated human Treg cells

PBMCs were isolated from fresh blood by differential density centrifugation using Ficoll-PLUS (GE Healthcare). Cells were washed three times in 1 % RPMI, then resuspended in PBS + 2 % HI-FCS + 2.0 mM EDTA (isolation buffer). $CD4^+$ $CD25^-$ and $CD4^+$ $CD25^+$ *T*-cells were isolated, per the manufacturer's instructions (Miltenyi $CD4^+$ $CD25^+$ Regulatory *T*-cell Isolation Kit, human). Isolated $CD4^+$ $CD25^-$ *T*-cells were then labeled with Cell Proliferation Dye eFluor® 450 per manufacturer's instructions (eBioscience). An aliquot of cells was stained with anti-CD3 and anti-CD4 (BioLegend and eBioscience) to assess cell purity and dye labeling by flow cytometry. Cultures were plated in cRPMI, with $2.5x10^4$ $CD4^+$ $CD25^-$ cells per well. Cells from the Treg cultures on day 10 were added to achieve a ratio of 1 effector: 2 Treg for all 3 donors. Anti-CD3/CD28 beads (Dynabeads® T Activator CD3/CD28 beads) were added at a 1:1 ratio with the total number of cells per well. Unstimulated $CD4^+$ $CD25^-$ *T*-cells and stimulated without Tregs were plated as controls. Where necessary, cRPMI was used to bring total culture volume to 200 μl. Cells were incubated for four days at 37 °C with 5 % CO_2. After four days, cells were stained with Fixable Viability Dye eFluor® 780 (eBioscience) for 30 min at 4 °C. Following staining, cells were washed and resuspended in PBS + 1 % HI-FCS (FACS buffer). Samples were run within four hours on a CyAn™ ADP Analyzer. Immediately prior to acquisition, cells were transferred to FACS tubes with an exact volume of CountBright™ Absolute Counting Beads (ThermoFisher Scientific). For the suppression assay, the absolute number of proliferating cells, the percentage of suppression compared to the stimulated *T*-cells without Tregs, and the suppression as a percentage of that achieved by Tregs cultured in the presence of vehicle, were determined and plotted as the mean and standard deviation of triplicate values, where adequate cell numbers were available. For the Treg induction cultures, the percentage of $Foxp3^+$ $CD25^+$ cells were reported, in addition to the percentage of $Foxp3^+$ $CD25^+$ cells as a percentage of the vehicle control. Graphs

represent values from individual cultures.

2.7. Mice

BALB/cAnNCrl mice were purchased from Charles River (Germany). The experiments were performed at Adlego Biomedical AB under the approval by the regional animal experimental ethics committee in Stockholm (North) (ethical permit N81/14).

C57BL/6(J) mice were purchased from Taconic M&B (Bomholt, Denmark) and experiments were performed upon approval by the regional Ethics Committees in Uppsala, Sweden (ethical permit C42/14 and 5.8.18–02686/2019). Housing conditions and experimental handling were performed according to the guidelines for animal experimentation and welfare at Uppsala University.

2.8. In vivo pharmacokinetic (PK) analysis of MALT1 inhibitor and IL-2 upon anti-CD3 challenge

Mouse plasma concentration of MALT1 inhibitor was measured upon administration of 30 μmol/kg of the compound given by oral gavage. Anti-CD3 injection solution was prepared by diluting 0.3 ml of CD3e monoclonal antibody (145-2C11) with 2.7 ml of sterile saline to make 3 ml of 0.1 mg/ml dosing solution. One hour prior to injection with the anti-CD3 antibody, female BALB/C mice (5–7 weeks old, 3 mice per group) were pre-treated with either vehicle (DMA: Solutol HS 15: 0.5 % PVP K30 (in PBS) = 1:5:4) or with MALT1 inhibitor compound given by oral gavage (30 μmol/kg body weight; 10 μl/g mouse gavage volume). At baseline blood was collected from the mice by submandibular bleeding (up to 150 μl/mouse). Sera were prepared immediately by centrifugation at 4 °C and stored at −80 °C. At baseline, the mice were subjected to a bolus tail vein injection of an anti-CD3e Monoclonal Antibody (145-2C11; 10 μg/mouse IV, 100 μl total volume of sterile saline). After 90 min (1.5 h) or four hours blood was collected following the anti-CD3 IV bolus as a terminal procedure by cardiac puncture. Isolated plasma was used for PK analysis and sera for multiplex cytokine analysis (MSD U-plex mouse Th1/Th2 combo (9 cytokines incl. IL-2, IFNγ) (K15071K-1)). Sera were immediately recovered from an aliquot of the collected blood by allowing the blood to clot at room temperature for 15–30 min in a vacutainer blood collection tube. The clot was removed by centrifugation at 2000xg at 4 °C for 10 min. The resulting supernatant (serum) was collected and immediately transferred to a clean tube that was aliquoted and stored in freezer for later analyses.

2.9. Four- and ten-day dosing treatment schemes with MALT1 inhibitor

For in vivo investigation of the effects of 4-doses orally administered MALT1 inhibitor on lymphocyte populations and safety in tumor bearing animals, MB49 cells ($3x10^5$ cells in 100 μl PBS) were subcutaneously (SC) injected in the flanks of C57BL/6 female mice that were subsequently separated to four groups of six mice each. Intravenous injections of anti-CD25, 200 μg (clone: PC61) were administered at day 8 and 11. Oral gavage treatments of vehicle control formulation, MALT1 inhibitor compound 3 μmol/kg (1.34 mg/kg) or 30 μmol/kg (13.4 mg/kg) were administered at day 8, 9, 10, 11 post tumor inoculation. At day 12, the animals were sacrificed and tumors, draining and non-draining side inguinal lymph nodes were harvested and preserved in RPMI on ice until processing. The tumors were cut into small pieces with blades, and treatment with Liberase™ TL Research Grade low Thermolysin concentration was used prior mechanic tumor cell dissociation. The tumors were incubated for 15 min at 37 °C. Enzymatic activity was stopped by the addition of 200 mM EDTA in PBS (final concentration 10 mM). Mesh membranes were used for mechanical dissociation of whole lymph nodes and Liberase-treated tumors. The membranes were moistened and cells were pressed through using the bottoms of 5 ml syringe and rinsed with 10 ml RPMI with 10 mM EDTA. Cell suspensions were centrifuged for 5 min at 1500 rpm and resuspended in PBS. For multicolor flow cytometry analysis appropriate volumes of single cell suspensions were incubated with 1 μl Purified anti-mouse CD16/32 Antibody (Biolegend, 101301) for Fc receptor blocking and then stained for extracellular markers with CD3-BV421 (100228), CD8-FITC (100706), CD4-PE (116005), CD25-PerCP Cy5.5 (101912, clone 3C7), all purchased from Biolegend. Following extracellular staining the FOXP3 Fix/Perm Buffer Set (421403) from Biolegend was used for FoxP3-AF647 (320014) staining according to the manufacturer's instruction.

For the in vivo assessment of tumor growth control by a 10-dose MALT1 inhibitor monotherapy, MB49 cells ($3x10^5$ cells in 100 μl PBS) were SC injected in the flanks of C57BL/6 female mice that were subsequently separated into three groups of 13 mice each. Oral gavage treatments of vehicle control formulation or MALT1 inhibitor at 30 μmol/kg or 30 μmol/kg were administered at days 11–15 and 18–22 post tumor inoculation. At day 15 four mice per group were sacrificed, tumors and draining side inguinal lymph nodes were harvested. The tissues were processed and stained as described above. Twice weekly the remaining 9 mice per group were monitored, weighed and tumors measured until day 47. Animals that had to be sacrificed due to tumor ulcerations when tumors were less than 0.8 mm^3 were excluded from the survival analysis and tumor size graphs.

2.10. MALT1 inhibitor treatment combination with anti-CTLA-4 immunotherapy

MB49 cells ($2x10^5$ cells in 100 μl PBS) were SC injected in the flanks of C57BL/6 female mice that were subsequently separated into four groups of 10 mice each. The administration of treatments and tumor measurements were performed as a blinded experiment. The four groups were treated with 1) PBS Control peritumoral (50 μl per animal) and vehicle control formulation, 2) MV088428 30 μmol/kg, 3) vehicle control formulation + anti-CTLA4 (9D9, BioXCell) 100 μg intraperitoneally, 4) MV088428 30 μmol/kg + anti-CTLA4 (9D9, BioXCell) 100 μg intraperitoneally. The injection treatments were administered on day 7, 10 and 13 post tumor inoculation, while the oral administration of vehicle control formulation or MALT1 inhibitor was performed daily from day 7 to 21 post tumor inoculation. Tumor measurement was performed from day 6, twice a week until day 76 which was the experimental endpoint. One mouse in the group receiving oral gavage of vehicle control formulation and anti-CTLA4 was sacrificed at day 12 due to signs of discomfort reaching the humane endpoint and was therefore excluded from the survival analysis.

2.11. MALT1 inhibitor treatment with interruption time-points

MB49 cells ($2x10^5$ cells in 100 μl PBS) were SC injected in the flanks of 38 C57BL/6 female mice. The animals received treatment composed of four orally administered MALT1 inhibitor doses of 30 μmol/kg or vehicle control formulation from day 7 to 10. The tumors and draining side inguinal lymph nodes were harvested for analysis after one day (n = 5 MV088428, n = 4 vehicle), three days (n = 5 MV088428, n = 5 vehicle), six days (n = 4 MV088428, n = 5 vehicle) or eleven days (n = 5 MV088428, n = 5 vehicle) since treatment interruption. The tissues were processed and stained for flow cytometry analysis as described above. Viability staining was performed with the Zombie Aqua™ Fixable Viability Kit (423101) from Biolegend according to the manufacturer's instructions. The following extracellular markers were used in a staining panel for natural killer (NK) cell, myeloid cell and IFNγ analysis: CD3 APC/Cy7 (100221, Biolegend), NK1.1 PE (108707, Biolegend), CD69 BV605 (563290, H1.2F3, BD), CD11B APC (101212, Biolegend), CD11C Alexa Fluor 488 (117311, Biolegend), Ly6C PerCP/Cy5.5 (128012, Biolegend), Ly6G BV785 (127645, Biolegend), CD8a PE/Cy7 (100722, Biolegend), MHCII BV650 (563415, BD) with intracellular IFNγ BV421 staining that was performed with the Fixation/Permeabilization BD kit (554714).

Among viable cells, NK cells were gated as $CD3^-$ $NK1.1^+$ cells, activated NK cells as $CD3^-$ $NK1.1^+$ $CD69^+$ cells, conventional dendritic cells (DCs) as $CD3^-$, $CD11b^+$, $CD11c^+$, MHC II^+, $CD8^-$ cells, plasmacytoid DCs as $CD3^-$, $CD11b^-$, $CD11c^+$, MHC II^+, $CD8^+$ cells and Monocytic myeloid derived suppressor cells (MDSCs) as $CD3^-$, $CD11b^+$, $CD11c^-$, $Ly6G^-$, $Ly6C^+$ cells. For analysis of *T*-cell subsets the following extracellular marker antibodies were used: CD3 APC/Cy7 (100221, Biolegend), CD4 PerCp/Cy5.5 (116012, Biolegend), CD8 PE/Cy7 (100722, Biolegend), CD44 BV785 (103041, Biolegend), CD62L BV605 (104438, Biolegend), CD25 Alexa Fluor 647 (563598, BD) with intracellular staining antibodies IFNγ BV650 (563854, BD), Ki67 PE (12–5698-82, eBioscience) and FoxP3 BV421 (562996, BD) that was performed with eBioscience kit for fixation/permeabilization (00–5523-00). The gating analysis strategy for the T cell subsets was as follows: Among $CD3^+$ $CD4^+$ or $CD3^+$ $CD8^+$ viable cells, the $CD25^+$ $Foxp3^+$ cells were defined as Treg, the $CD44^-$ $CD62L^+$ as Naïve *T*-cells, the $CD44^+$ $CD62L^-$ as Effector memory *T*-cells and the $CD44^+$ $CD62L^+$ as Central memory *T*-cells.

2.12. Adoptive T cell transfer

PMEL $CD8^+$ *T*-cells (gp100 specific) ($10x10^6$ cells in 100 μl PBS) from a Thy1.1 C57BL/6 background were injected intravenously to 34 healthy C57BL/6 female mice. On the same day the mice were injected in the foot pad with human gp100 short peptide KVPRNQDWL (100 μg in 20 μl PBS) (except for the group receiving only IL-2). Anti-CTLA4 (200 μg in 100 μl PBS, 9D9, BioXCell) was injected intravenously to the respective groups on days 0 and 3. IL-2 (20000 units in 100 μl PBS) was administered daily intraperitoneally (IP). Three or 30 μmol/kg of MALT1 inhibitor or vehicle control formulation were administered via oral gavage daily from day 0 to day 4. On day 5 the mice were sacrificed and the draining lymph nodes were harvested and analyzed by flow cytometry as described above.

The antibodies used for extracellular marker staining were CD4 FITC (116004, Biolegend), CD8 PE-Cy7 (100722, Biolegend), CD44 Bv785 (103041, Biolegend), CD62L APC (104412, Biolegend), CD25-PerCP Cy5.5 (101912, clone 3C7, Biolegend), Thy1.1 PE (202524, Biolegend, clone OX-7) and intracellular Foxp3 BV421 (562996, BD) staining was performed with the eBioscience kit for fixation/permeabilization (00–5523-00). The gating analysis strategy for the *T*-cell subsets involved the use of Fluorescence Minus One Control (FMO) and was set as follows: Among $CD3^+$ $CD4^+$ viable cells the $Foxp3^+$ cells were defined as Treg, and $Thy1.1^+$ cells among $CD8^+$ cells as antigen specific *T*-cells. Among $Thy1.1^+$ cells, $CD44^-$ $CD62L^+$ as Naïve *T*-cells, the $CD44^+$ $CD62L^-$ as Effector memory *T*-cells and the $CD44^+$ $CD62L^+$ as Central memory *T*-cells.

2.13. Statistical analysis

Kruskal-Wallis tests were used for multiple comparisons of data that did not follow Gaussian distribution, while for normally distributed data ordinary one-way ANOVA testing with Holm-Sidak correction for multiple testing was used. For analysis of repeated measures data, a mixed-effects model with Geisser-Greenhouse sphericity correction and Holm-Sidak correction for multiple comparisons was used. Error bars represent standard deviation. The statistical significance of survival curves was determined by Log-rank (Mantel-Cox) testing. Graphical illustrations of experimental procedures were created with BioRender.com and graphs generated with GraphPad Prism 9.3.0.

3. Results

3.1. In vitro cellular effects of MALT1 inhibitor on MALT1 substrate cleavage and IL-2 secretion

In order to examine the in vitro downstream effects of the MALT1 inhibitor, cells with intact MALT1 signaling were used. Jurkat cells were exposed to escalating doses of inhibitor followed shortly by PMA/Ionomycin stimulation. In line with previous studies [19,20], cell lysates caused cleavage of HOIL1 (HOIL1 Cter), which was inhibited in response to the compound (Supplementary Fig. S1A, B). Based on these data, the EC50 was quantified at 12 nM. To further examine the effects of the compound on cell activation in vitro, Jurkat cells were stimulated with PMA/Ionomycin for 24 h. IL-2 secretion in stimulated Jurkat cells was ablated by MALT1 inhibition (Supplementary Fig. S1C), confirming similar findings of allosteric MALT1 inhibition [33,34]. In conclusion, in addition to HOIL1 cleavage inhibition, MALT1 inhibition impacted the capacity of an immortalized T cell line, Jurkat cells, to produce IL-2 upon in vitro stimulation.

3.2. In vitro inhibition of naïve T cell differentiation to Treg by MALT1 inhibition

A standard protocol of in vitro Treg differentiation (Fig. 1A) was used to examine the effects of the MALT1 inhibitor on differentiation of naïve $CD4^+$ *T*-cells to Tregs. Phenotypic analysis of the cells revealed that the presence of the inhibitor in the cell culture led to potent inhibition of $CD4^+$ *T*-cell differentiation to Treg (Fig. 1B-C). Moreover, the Treg mediated suppression of $CD4^+$ T effector cells (co-culture of Treg:Teff cells) was significantly decreased compared to T effector cells co-cultured with Treg in the absence of MALT1 inhibitor (Fig. 1D).

3.3. Pharmacokinetic and pharmacodynamic studies of MALT1 inhibition in vivo

The pharmacokinetic profile of the MALT1 inhibitor at time points between 15 and 120 min is shown in Fig. 2A.

Having confirmed the efficacy of the compound in vitro, we moved on to examine how the inhibitor modulates cytokine release in vivo. First an experiment with tumor-free mice was performed to examine how the inhibitor modulates cytokine release following injection with an anti-CD3 antibody, and the relationship to exposure levels. (Fig. 2B). Levels of mIL-2 were not measurable after only a 1.5-hour anti-CD3 challenge. Serum concentrations of mIL-2 upon 4 h of anti-CD3 challenge were impacted when mice were pre-treated with MALT1 inhibitor (mean 513 pg/μl, SD 171) compared with mice pre-treated with vehicle control formulation (mean 3077 pg/μl, SD 385) (Fig. 2C) Analysis of the free plasma concentration of MALT1 inhibitor indicated that exposure was the same at both time-points (1.5 hr mean 9.361 μM, SD 1.543 and 4 hr mean 11.60 μM, SD 2.092) (Fig. 2D).

3.4. No tumor growth control or improved survival by MALT1 inhibition in vivo

To examine the ability of the MALT1 inhibitor to reduce Treg frequencies in tumor bearing animals, the MB49 urothelial cancer cell line was engrafted and treatment was performed as indicated in the graph (Fig. 3A). A short-interval daily treatment period (4 days) was followed by tumor measurement and flow cytometry analysis of tumors and inguinal lymph nodes at day 12. The short-interval treatment did not reduce tumor growth at this timepoint compared to vehicle-treated animals (Fig. 3B), and no significant Treg frequency reduction was observed in tumors (Fig. 3C), despite the observed dose-dependent inhibition of Tregs in the lymph nodes (Fig. 3D, E). Anti-CD25 therapy targeting the IL-2 receptor was used as a positive control for partial Treg depletion, but the dose of anti-CD25 that was used did not reduce Treg frequencies significantly in lymph nodes when compared to vehicle treated mice (Fig. 3D, E). In contrast, the frequencies of $CD4^+$ T effector cells and $CD8^+$ *T*-cells were decreased in tumors and non-draining lymph nodes, respectively, by anti-CD25 therapy (Fig. 3 F, N). The numbers of intra-tumoral $CD4^+$ and $CD8^+$ *T*-cells were reduced in animals treated with the highest dose of MALT1 inhibitor (Fig. 3 I, L).

Based on the reduction of Treg in the lymph nodes, the lack of side

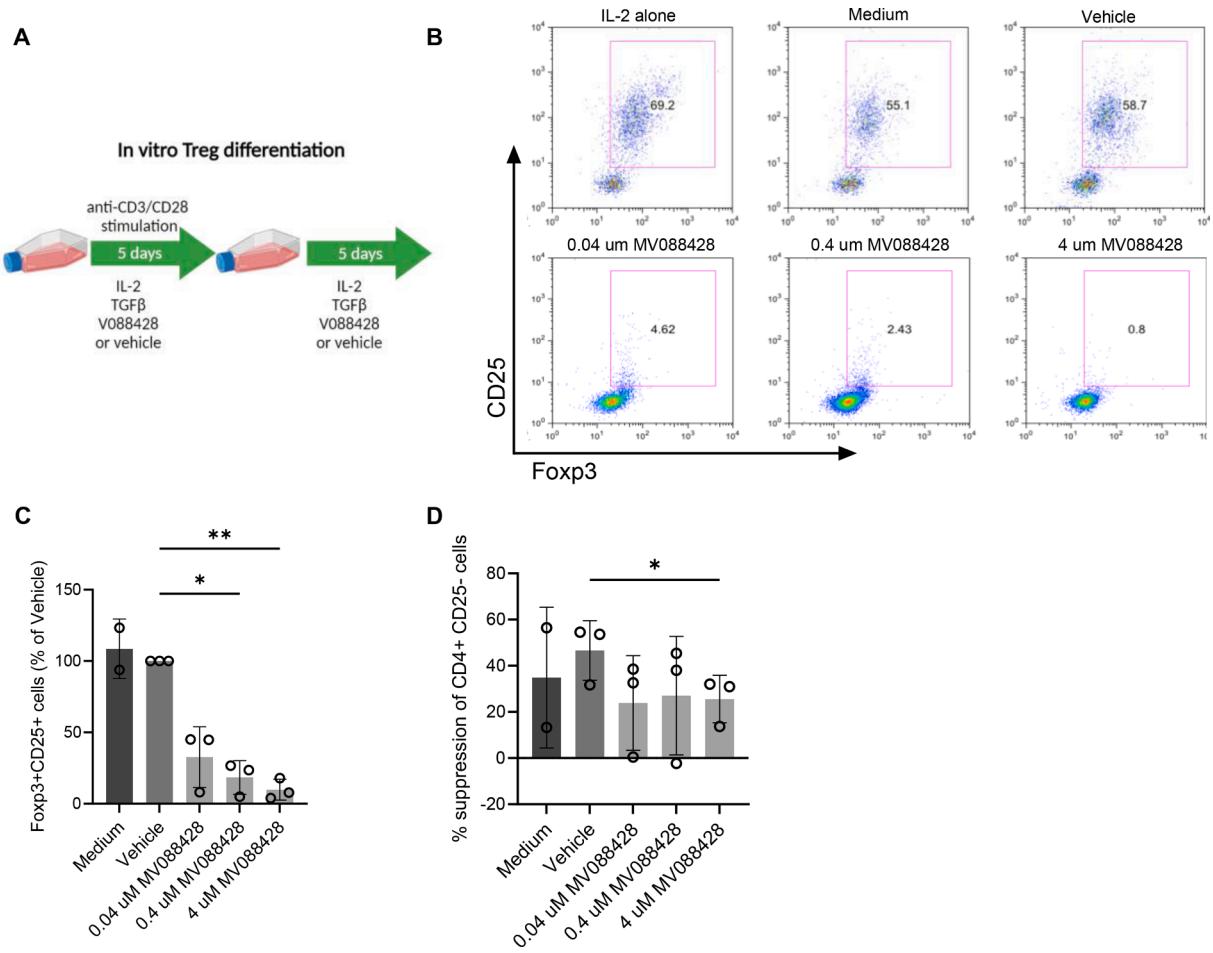

Fig. 1. Assessment of the impact of MALT1 inhibition on Treg differentiation in vitro. (A) Schematic of the Treg in vitro differentiation protocol using peripheral blood from healthy donors. (B) Representative scatter-plot for one donor. (C) Treg levels after MALT1i shown as % of vehicle. Compound MV088428 inhibited TGF- beta/IL-2-dependent in vitro Treg differentiation following CD3/CD28 bead stimulation. (D) Suppression of CD3/CD28 stimulated CD4 + T effector cells (CD4+/CD25-) by in vitro differentiated Treg cells was assessed after 4 days. Statistical assessment by One/Two-Way ANOVA. Mean percentage +/- SD.

effects and to pursue an anti-tumor effect by prolonging the suppression of Tregs, a longer treatment scheme was applied starting at 11 days post MB49 tumor cell inoculation (2 weeks of treatments in a scheme of 5 days treatment, 2 days pause, 5 days treatment). However, the animals that were exposed to the longer treatment strategy did not exhibit tumor growth control or improved survival compared to vehicle treated mice (Fig. 4 A-E), neither were *T*-cell subsets further affected by longer treatment (Tregs shown in Figure F-G; other *T*-cell subsets not shown). No direct side effects were observed during any of the monitoring periods and no macroscopic pathologic findings were identified at necropsy of the tumor bearing animals (data not shown).

3.5. MALT1 inhibition attenuates the anti-tumor efficacy of anti-CTLA4 checkpoint blockade

As MALT1 inhibition caused a reduction of peripheral Tregs in tumor bearing animals but failed to impact on tumor growth, we designed a combination treatment experiment with anti-CTLA4 to examine whether this could improve anti-tumor efficacy. Animals were treated daily with vehicle or 30 μmol/kg of MALT1 inhibitor from day 7–21 post tumor inoculation, while three doses of 100 μg anti-CTLA4 or control PBS were administered at days 7, 10 and 13 (Fig. 5A). Tumor measurements were performed twice weekly until day 80. Surprisingly, the combination treatment abolished the therapeutic efficacy of anti-CTLA4, resulting in decreased overall survival as a result of tumor growth (Fig. 5B, F).

3.6. No change in frequencies of major immune cell subsets by MALT1 inhibition in lymph nodes

As the addition of MALT1 inhibition to anti-CTLA4 immunotherapy depleted the effect of anti-CTLA4, we speculated that other immune cell populations may be affected by the treatment.

With that in mind, we performed a detailed flow cytometry analysis to study the effect of MALT1 inhibition on a number of immune cell subsets in draining lymph nodes (Supplementary Fig. S2). As in our previous experiments (Fig. 3), the MALT1 inhibition-mediated decrease of Treg in lymph nodes is maintained between short (4 days) and long (2 weeks) treatment periods. Thus, the short period treatment experiment composed of four inhibitor doses of 30 μmol/kg was repeated. The lymph nodes were harvested for analysis after one, three, six or eleven days of treatment interruption (Supplementary Fig. S2A). The percentages of *T*-cells with phenotypes of proliferating, Naïve, effector (IFN-γ-producing) memory, or central memory $CD4^+$ and $CD8^+$ *T*-cells remained unchanged (no statistically significant changes) between treated and untreated mice for each timepoint post treatment interruption (Supplementary Fig. S2B-K). Furthermore, analysis of all NK cells ($CD3^-$ $NK1.1^+$) and activated NK cells ($CD3^-$ $NK1.1^+$ $CD69^+$), as well as analysis of conventional DCs ($CD3^-$ $CD11b^+$ $CD11c^+$ MHC II^+ $CD8^-$), plasmacytoid DCs ($CD3^-$ $CD11b^-$ $CD11c^+$ MHC II^+ $CD8^+$) and monocytic MDSCs ($CD3^-$ $CD11b^+$ $CD11c^-$ $Ly6G^-$ $Ly6C^+$) showed no significantly altered cell frequencies between tumors or lymph nodes of treated and untreated animals. As expected, Treg levels were

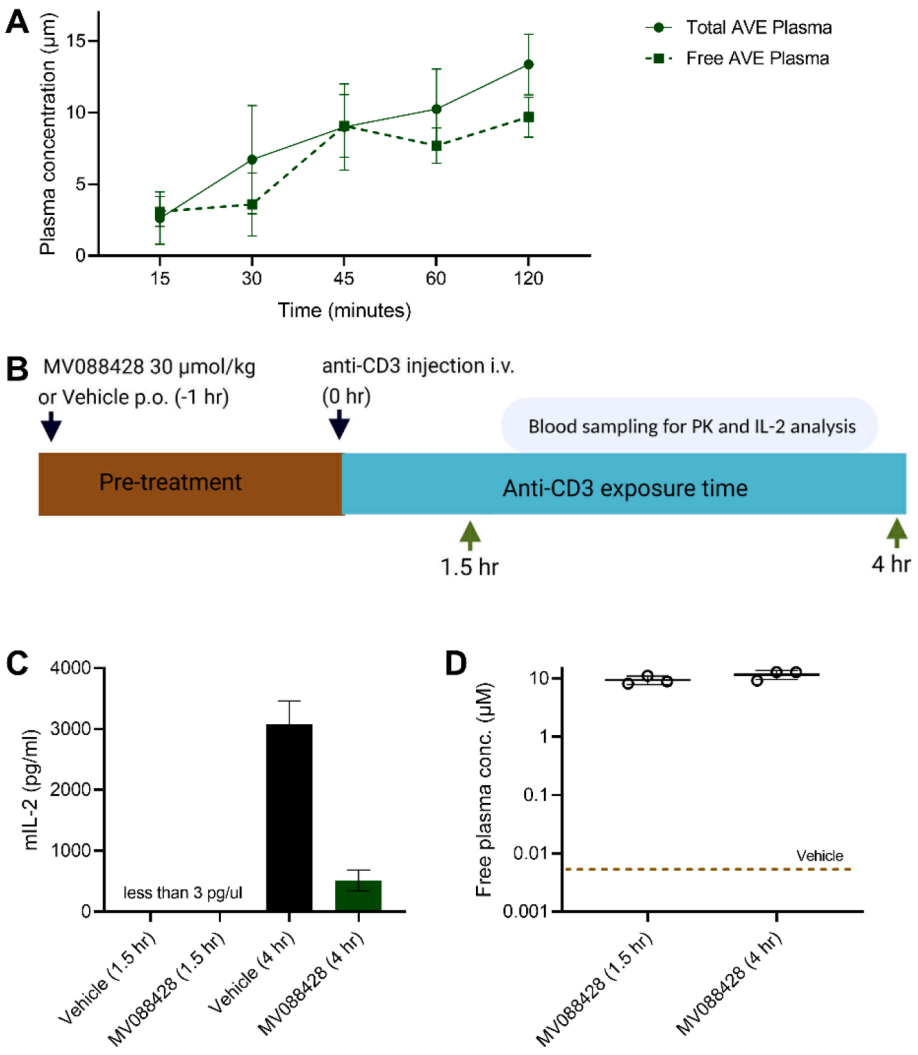

Fig. 2. MALT1 inhibition blocks serum IL-2 release in vivo following anti-CD3 challenge. BALB/cAnNCrl mice were used in this experiment. (A) PK profile of the MALT1 inhibitor showing total and free plasma concentration. (B) Schematic of in vivo experiment. (C) Mouse serum IL-2 levels 1.5 and 4 hr after anti-CD3 treatment in the presence and absence (vehicle) of MALT1 inhibitor (MV088428). Average of N = 3 is shown +/ SD. (D) Free plasma concentration of inhibitor in mouse plasma at 1.5 and 4 hr following anti-CD3 in relation to Ki. Median of an N = 3/time point is shown.

significantly decreased one day after a cycle of therapy (Supplementary Fig. S3).

3.7. Suppression of antigen-specific T cells by MALT1 inhibition in the presence of anti-CTLA4

Since MALT1 inhibition monotherapy did not affect the frequencies of any of the major *T*-cell subsets except for Tregs, we pursued to investigate the effect of combined MALT1 / anti-CTLA4 treatment on antigen-induced *T*-cell expansion in the lymph nodes. To that end, PMEL $CD8^+$ $Thy1.1^+$ *T*-cells were injected in tumor free mice with co-administration of hgp100 short peptide, anti-CTLA4 and IL-2 (Fig. 6A). On day 5 the mice were sacrificed and cell populations in the draining lymph nodes were analyzed by flow cytometry. As in the previous experiments, Treg- frequencies were reduced in presence of MALT1 inhibitor (Fig. 6C), while the total numbers of $CD8^+$ *T*-cells, naïve $CD8^+$ and effector memory $CD8^+$ *T*-cells remained unchanged between vehicle and inhibitor treated animals (Fig. 6D, F-H). In the presence of anti-CTLA4 and upon antigen-stimulation, the addition of MALT1 inhibition substantially affected the frequency of $Thy1.1^+$ hg100 antigen specific $CD8^+$ *T*-cells (gated as in Fig. 6B) in lymph nodes, regardless of IL-2 co-administration (Fig. 6E). These results suggest that although the MALT1 inhibitor did not appear to impact the frequencies of naïve and memory *T*-cell subsets, there was a notable impact on the frequency of antigen-specific *T*-cells when the MALT1 inhibitor was administered during antigen-exposure. Moreover, it appears that co-administration of IL-2 was not sufficient to reverse this effect, although the chosen IL-2 dose, due to its short half-life, may have been insufficient to elicit a full rescue of the antigen-induced proliferation

4. Discussion

A high frequency of infiltrating Treg cells along with low $CD8^+$ *T*-cell frequencies in tumors correlate with a poor prognosis [35,36], and there is growing evidence that removal of Tregs enhances anti-tumor immune responses. A critical role of NF-κB signaling in Treg differentiation and function has recently been established, making it an interesting target for tumor immunotherapy. To this end, inhibition of components of the CBM complex, such as MALT1, has been exploited in several studies [37].

We investigated the impact of MALT1-inhibition in a murine model of urothelial cancer: C57BL/6 mice inoculated with MB49 cancer cells. The relevance of this model is supported by findings of infiltration of $FoxP3^+$ Tregs in human bladder carcinoma [38] and an association between poor prognosis of non-muscle-invasive bladder cancer and infiltration of $Foxp3^+$ T cells that suppress anti-tumor immunity [39].

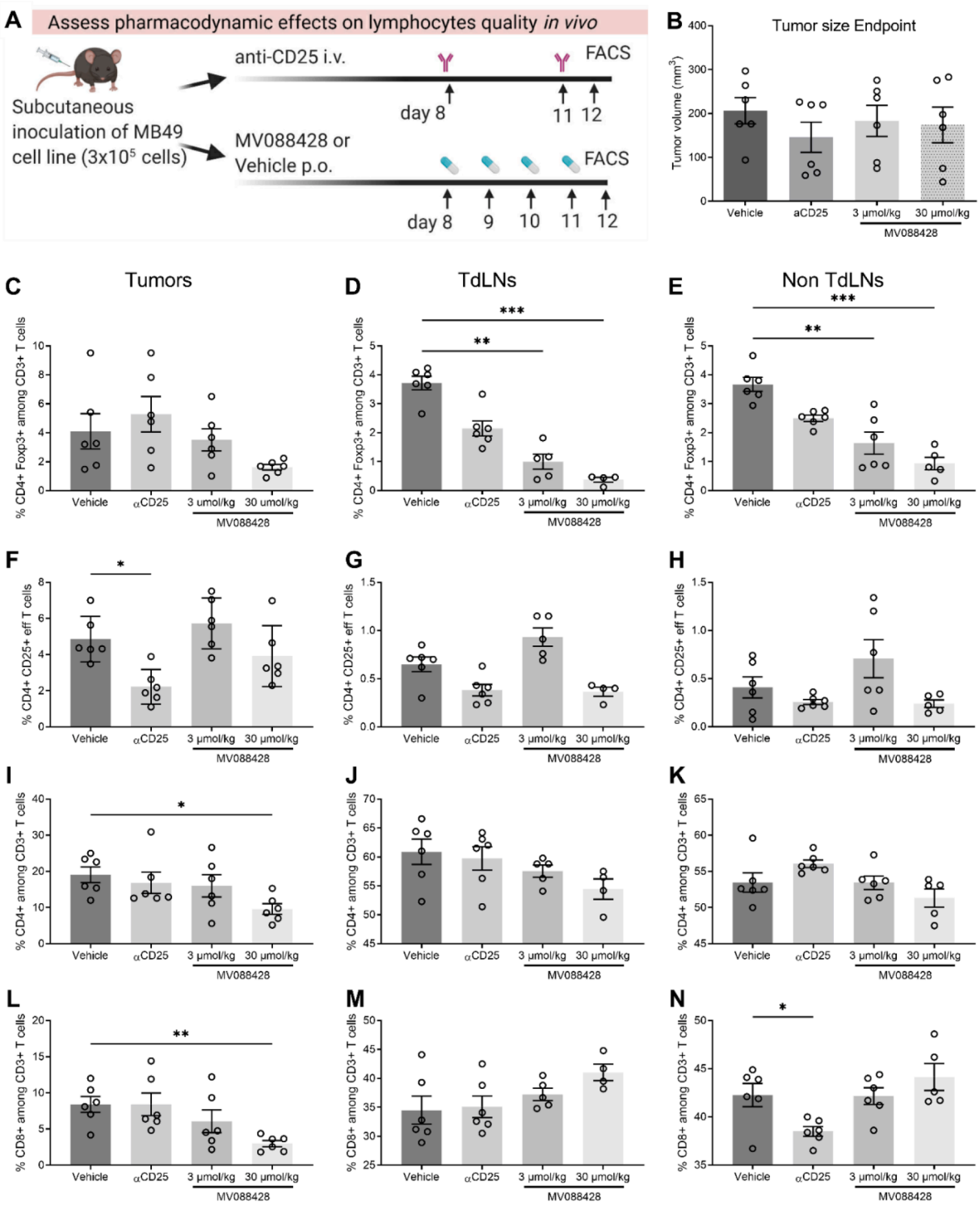

Fig. 3. MALT1 inhibition reduces the frequencies of Tregs in lymph nodes without inhibiting tumor growth after a short treatment period. C57BL/6 mice were inoculated SC with MB49 cancer cells. MALT1 inhibitor was administered as oral gavage (OG) on days 8–11 after tumor inoculation. Anti-CD25 antibody was administered intravenously on day 8 and day 11. On day 12 the mice were sacrificed and the tumor and LNs were analyzed with flow cytometry (A). Tumor volume on day 12 after tumor inoculation (B). Frequency of Tregs among CD3 + T cells, CD4 + CD25 + effector T cells, conventional CD4 + and CD8 + T cells in tumors, draining lymph nodes (TdLN) and non-draining lymph nodes (Non TdLN) (C—N).

Initial experiments in vitro were performed to confirm the efficacy of the inhibitor used in this study. Indeed, the MALT1 inhibitor suppressed proteolytic cleavage of the MALT1 substrate HOIL1 in Jurkat cells. Moreover, the MALT1 inhibitor suppressed the in vitro proliferation of $CD4^{+}$ $FoxP3^{+}$ positive Tregs. There are conflicting results regarding the effect of MALT1-inhibitors on Treg proliferation, depending on the selection of compound: whereas the allosteric MALT1 inhibitor mepazine did not affect T reg differentiation in vitro [40], the more potent inhibitor MLT-985 was associated with a rapid and dose dependent reduction in Tregs [41]. The MALT1-inhibitor used in our study is highly selective, and with a IC_{50} in the nanomolar range, significantly more potent than mepazine. Interestingly, Biswas *et al* demonstrated in a rat

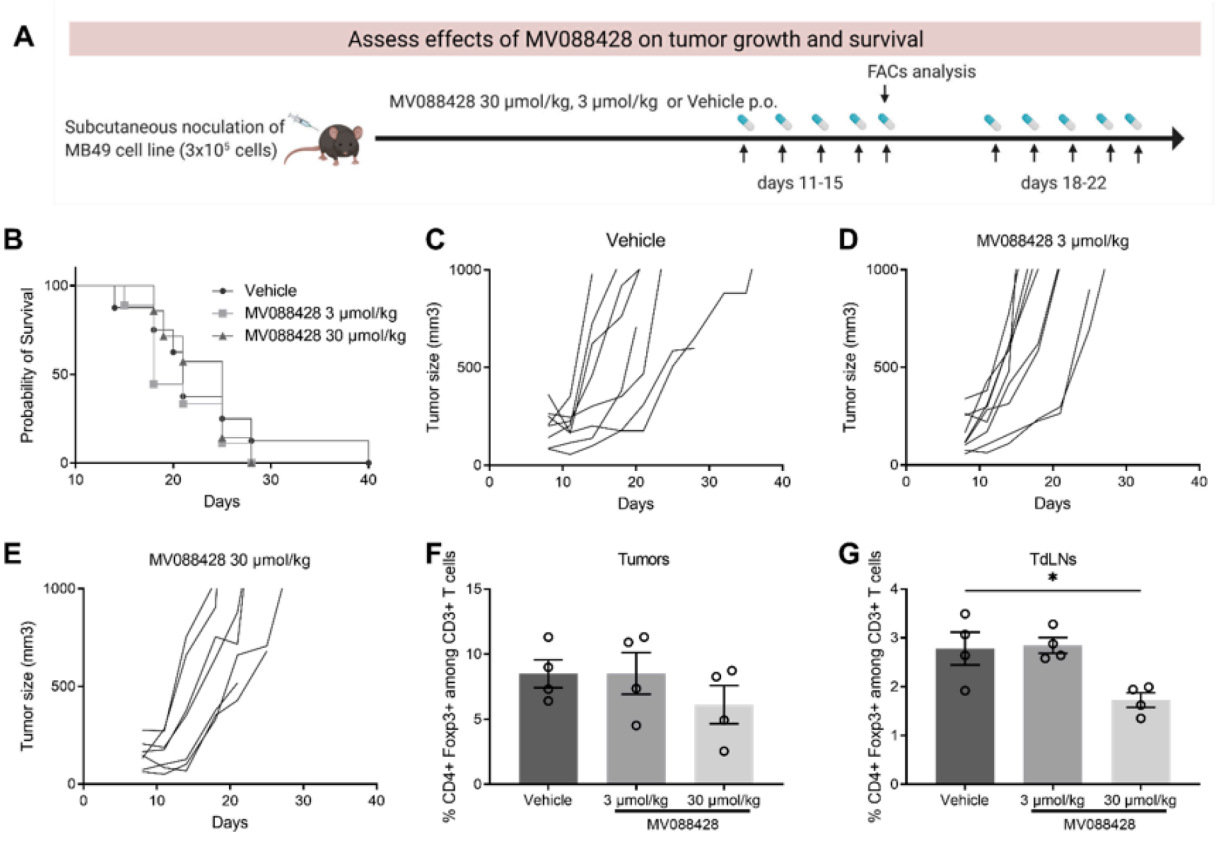

Fig. 4. MALT1 inhibitor reduces the frequencies of Tregs in lymph nodes without inhibiting tumor growth after a 10-dose treatment period. C57BL/6 mice were inoculated SC with MB49 cancer cells. The inhibitor was administered as oral gavage (OG) on days 8–11 after tumor inoculation. On day 15 four mice per group were sacrificed and the tumor and LNs were analyzed with flow cytometry (A). Survival analysis (B). Tumor volume size graphs (C-E). Frequency of Tregs among CD3 + T cells in tumors and draining lymph nodes (TdLNs) (F-G).

collagen-induced arthritis model that the effect of MALT1-inhibition is highly dose-dependent. They observed statistically significant decreases in Treg numbers at the highest dose of inhibitor, but by decreasing the dose 3 to 5 times this effect was lost, while keeping the efficacy in reducing disease severity of the autoimmune joint inflammation [34].

We also confirmed that anti-CD3- induced IL-2 secretion was suppressed both in vitro and in vivo, investigating tumor-free C57BL/6 mice.

In the MB49 tumor bearing mice, a selective Treg reduction in the tumor draining and non-tumor draining lymph nodes was noted after 4 days of treatment, while no effect was observed on conventional $CD4^+$ and $CD8^+$ *T*-cells in the lymph nodes. However, despite the selective impact on Treg levels in the lymph nodes there was no evident anti-tumor effect even after 10 days of treatment. Interestingly, $CD4^+$ and $CD8^+$ *T*-cell frequencies were reduced in tumors after 4 days of treatment, whereas Tregs in the tumors were unaffected by MALT1-inhibition. This puts into question the Treg-specificity of MALT1-inhibition in our setting with pharmacologic blocking, in contrast to previous reports where MALT1-inhibition was performed specifically in Tregs [24,28]. MALT1 inhibitors may also affect conventional *T*-cells, antigen-presenting cells, and other tumor microenvironmental cells. A possible explanation of the lack of anti-tumor effect in our model may be that not only Tregs were suppressed by MALT1 inhibition. The demonstrated reduction of anti-CD3- induced IL-2 secretion in our study is an indication of suppressed effector *T*-cells as Tregs do not themselves produce IL-2 [42].

To understand the role of immune cell contexture post MALT1 inhibitor administration we treated tumor bearing animals with the inhibitor or vehicle control and analyzed the Treg levels in lymph nodes, as well as NK cells, conventional DCs and monocytic DCs at different time points after therapy. While Treg reduction was apparent, there were no significant changes in these other cell subsets when compared to the vehicle control. However, the analysis of immune cell subtypes in our study was limited to their immunophenotypic characterization, while methods such as CYTOF or scRNA sequencing analysis could provide more detailed information on their functional status. Thus, the lack of therapeutic effect and reduction of antigen-specific *T*-cell frequency by MALT1 inhibition could be further investigated, and possibilities such as impairment of cytokine secretion, receptor dysregulation or antigen processing and presentation addressed.

Tumor-infiltrating Tregs express high levels of CTLA-4, which may contribute to Treg-mediated immune suppression. With this in mind, we assessed MALT1 inhibition in combination with systemic anti-CTLA4 therapy. In a previous study using the MB49-model, we showed that the tumor-suppressive effect of monotherapy with anti-CTLA-4 was mediated through T effector cells, whereas it had limited effects on the Treg compartment [43]. However, we and others have noted that anti-CTLA-4 in combination with stimulating therapies impacts on both Tregs and T effector cells with synergistic effects on anti-tumor efficacy [43,44]. But instead of the expected synergistic effect of MALT1- and checkpoint inhibition in the present study, it was apparent that long-term MALT1 inhibition negatively impacted the efficacy of anti-CTLA4 therapy. This suggests that MALT1-inhibition abolished the effect of systemic anti-CTLA-4 therapy on T effector cells, overshadowing any positive effect it may have had on the Tregs. In line with this, CTLA-4-blockade on T effector cells alone had a positive effect on survival in a mouse model of humanized CTLA-4, whereas unicompartmental blockade on Tregs failed to improve the anti-tumor responses [44].

Previous published work using pharmacological inhibition of MALT1 in solid tumors have focused mainly on its role of converting Tregs into

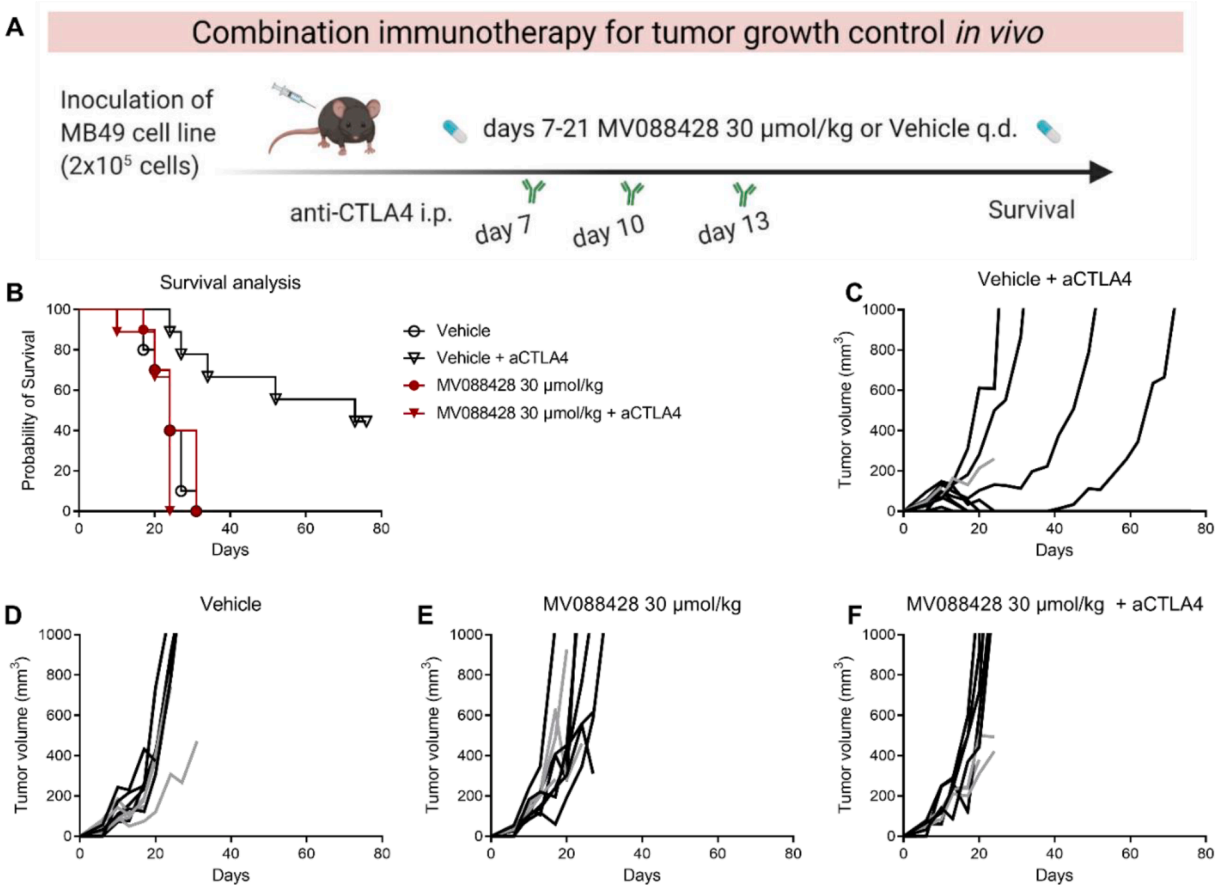

Fig. 5. MALT1 inhibition in combination with anti-CTLA4 attenuates the therapeutic anti-tumor effect of anti-CTLA4 checkpoint inhibition. MB49 tumor cells were inoculated SC to C57BL/6 mice which comprised four groups of 10 animals. Treatment with MALT1 inhibitor or vehicle was orally administered from day 7 to 21 post tumor inoculation. Mice were treated IP with anti-CTLA4 on days 7, 10 and 13 post tumor inoculation (A). Survival analysis (B) and tumor size (C-F). Grey lines indicate animals that reach the humane endpoint due to tumor ulceration and not due to tumor size.

effector cells and the synergistic effect of combined MALT1- and PD1-inhibition [26,27]. In contrast, CTLA-4 blockade aids to release breaks in early *T*-cell priming, leading to a polyclonal T cell response and is therefore more likely to be dependent on antigen-presentation/early T cell priming for its effect. MB49 cells are responsive to anti-PD1 therapy, and we have previously shown that subtherapeutic doses of anti-PD1 and anti-CTLA-4 in combination leads to synergistic effects in the MB49 model [45]. In the present study using the MB49 model we therefore also explored a subtherapeutic dose of anti-PD1 therapy combined with the optimal dose of MALT1 inhibition. We did not note a synergy of this combination, but in line with previous data, we also did not see any negative influence of MALT1-inhibition on anti-PD1 therapy (not shown). An optimal high dose of anti-PD1 therapy in combination with MALT1 inhibition was not explored herein. The contrasting data found between anti-PD1 therapy combined with MALT1 inhibition could be due to the mechanism of action targeting PD1/PDL1 versus CTLA-4, along with differences in the adaptive immunity of the tumor models explored. Since anti-CTLA-4 therapy harnesses and aids early T cell priming and T cell diversity, MALT1 could be essential for this effect, while anti-PD1 therapy mainly supports the rescue of already primed but exhausted tumor-reactive T cells to promote clonal expansion of those cells. Our data on the negative impact on T cell priming also supports this differentiation and can explain the results herein.

Intriguingly, there is evidence that MALT1 proteolytic activity is involved in the regulation of additional kinase pathways beyond NF-κB, such as JNK [18] and mTOR [46] as well as in mRNA stability via proteolysis of mRNA-destabilizing proteins roquin and regnase-1 [47]. Hence it is likely that MALT1 inhibition can affect many other TCR-driven immunological responses. We therefore examined the effects of our MALT1 inhibitor on antigen-specific T cells in the lymph nodes in combination with anti-CTLA-4 therapy during peptide antigen-stimulation. We found that MALT1 inhibition reduced the expansion of antigen-specific $CD8^+$ *T*-cells and that the effect could not be rescued by a daily IP injection of IL-2. Thus, while MALT1 inhibition reduced Treg frequencies in lymph nodes, it is possible that the negative impact of MALT1 inhibition on antigen-specific induced *T*-cell proliferation can counteract any positive effect from Treg inhibition. As such it could be preferred to develop pro-drug MALT1 inhibitor conjugates that can be targeted and internalized into Tregs to optimize the use of MALT1 inhibitors as immunotherapeutic agents. Alternatively, sequential dosing schedules could be investigated to avoid the presence of MALT1 inhibition during antigen-presentation and *T*-cell proliferation phases.

In conclusion, MALT1- inhibition resulted in reduction of Tregs in lymph nodes of MB49 tumor bearing animals as well as reduction of antigen-specific $CD8^+$ *T*-cell frequencies in an adoptive *T*-cell transfer model. The potential effects of MALT1 inhibition on general immunosurveillance that depend on *T*-cell priming and proliferation should be considered when planning efficacy studies for lymphomas and solid tumors. The negative effect MALT1 inhibition on CTLA-4 blockade also indicates that MALT1 inhibition plays a large role in antigen-specific priming and expansion. If the same mechanism is true for its impact on the Treg compartment, then the distinct profile/impact shown herein by MALT1 inhibition could be explained as follows; the Treg compartment in the draining lymph node that is affected by MALT1 inhibition largely consists of a thymic Tregs [48] i.e. cells that are in a proliferating state in response to tumor-antigen release and/or activating signals,

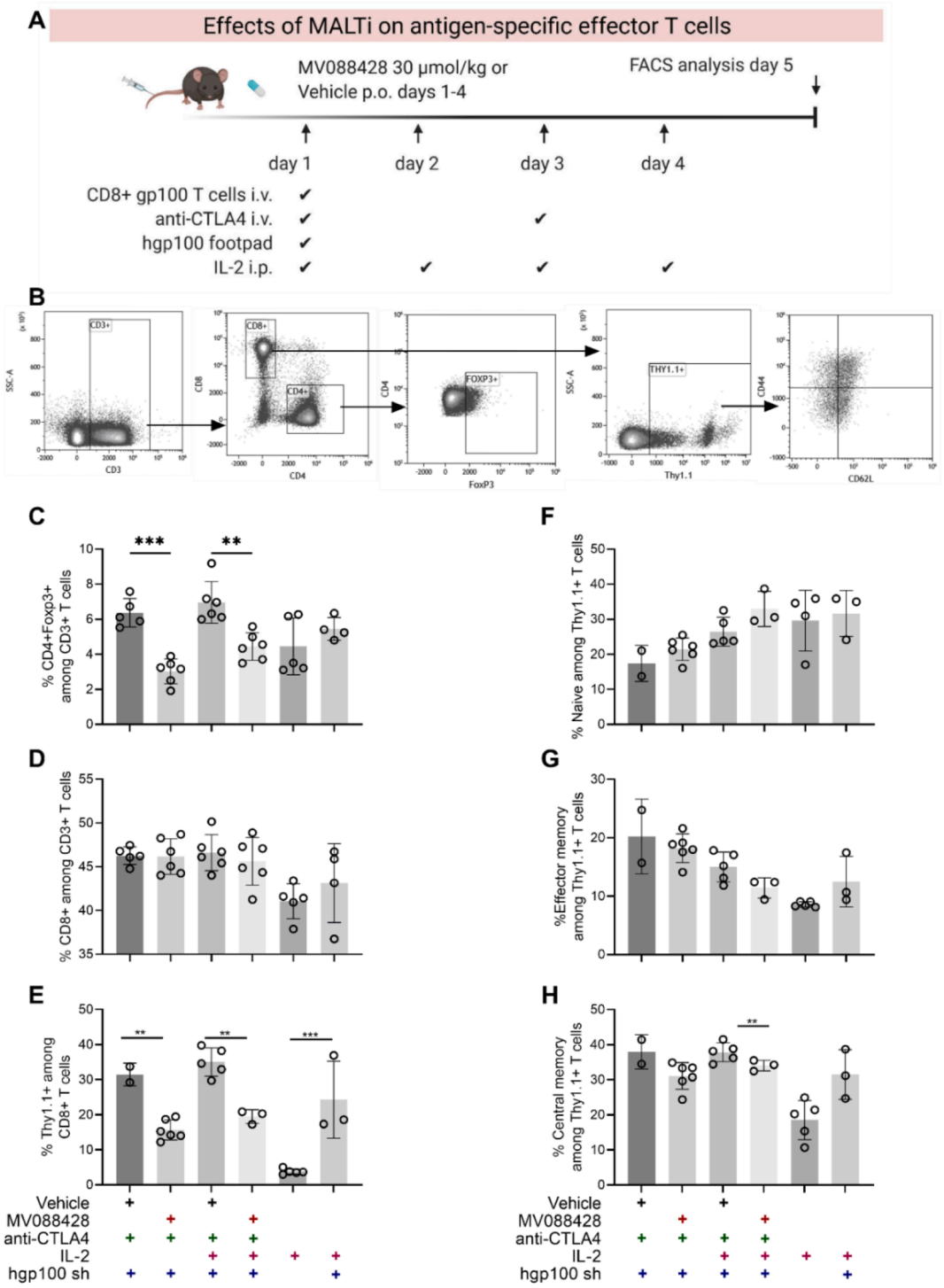

Fig. 6. MALT1 inhibitor reduces the frequency of antigen-specific T cells in the lymph nodes. PMEL CD8 + T cells were injected IV to C57BL/6 mice, and on the same day the mice were injected in the foot pad with Hgp100 short peptide (not in the IL-2 group). Anti-CTLA4 (200 µg) was administered on days 0 and 3, and IL-2 (20000 Units) was administered daily intraperitoneally. MALT1 inhibitor or vehicle was administered daily day 0 to day 4. On day 5 the mice were sacrificed and the dLN was analyzed with flow cytometry. Frequency of CD4 + Foxp3 + Tregs among CD3 + T cells (C). Frequencies of viable CD8 T cells (D), Thy1.1 antigen specific cells among CD8 + T cells (E) and naïve (CD44- CD62L +) (F), Effector memory (EM) (CD44 + CD62L-) (G) and Central memory (CM) cells (H) among Thy1.1 CD8 + T cells.

while the intratumoral Treg compartment, not affected by MALT1 inhibition, consists of non-proliferating peripheral or migrating Tregs [49]. Our study provides new insight into the risks of off-target effects of MALT1-inhibition on de novo *T*-cell generation, which could impact the long-term outcome for patients depending on the choice of combination therapy and/or tumor indication chosen for therapeutic intervention.

5. Institutional review board statement

The study involving human derived blood samples was conducted according to the guidelines of the Declaration of Helsinki by Celentyx Ltd, Birmingham Research Park, Vincent Drive, Edgbaston, Birmingham, West Midlands, B15 2SQ, UK, https://www.celentyx.com. The

study with BALB/cAnNCrl mice were performed under the approval by the regional animal experimental ethics committee in Stockholm (North) (ethical permit N81/14). Experiments with C57BL/6(J) mice were performed upon approval by the regional Ethics Committees in Uppsala, Sweden (ethical permit C42/14 and 5.8.18-02686/2019).

6. Author statement

I, Sara Mangsbo, certify that all **authors** have seen and approved the final version of the manuscript being submitted and warrant that the article is all uor original work and that it hasn't received prior publication and isn't under consideration for publication elsewhere.

7. Informed consent statement

Informed consent was obtained from all subjects involved in the study.

Funding

This research was supported by a grant from Medivir AB to Uppsala University, Sweden.

Conflicts of interest

The funding was obtained from Medivir and at the time of data generation **Anders Kallin, Niklas Finnberg, Karolina Ersmark, Mark Albertella and Fredrik Öberg** were employees of Medivir AB. Medivir AB as legal entity however had no role in the design of the study; in the collection, analyses, or interpretation of data; in the writing of the manuscript, or in the decision to publish the results. Aikaterini Nasi is a current employee of AstraZeneca.

CRediT authorship contribution statement

Iliana K. Kerzeli: Writing – review & editing, Writing – original draft, Visualization, Validation, Software, Resources, Project administration, Methodology, Investigation, Formal analysis, Data curation. **Aikaterini Nasi:** Resources, Methodology, Investigation. **Erika Fletcher:** Validation, Software, Resources, Methodology, Investigation, Formal analysis, Data curation. **Aikaterini Chourlia:** Resources, Methodology, Investigation. **Anders Kallin:** Methodology. **Niklas Finnberg:** Methodology, Formal analysis. **Karolina Ersmark:** Methodology, Formal analysis. **Maria Lampinen:** Writing – review & editing. **Mark Albertella:** Methodology, Formal analysis, Conceptualization. **Fredrik Öberg:** Visualization, Supervision, Resources, Methodology, Funding acquisition, Formal analysis, Conceptualization. **Sara M. Mangsbo:** Writing – original draft, Visualization, Supervision, Resources, Project administration, Methodology, Funding acquisition, Formal analysis, Conceptualization.

Declaration of Competing Interest

The authors declare that they have no known competing financial interests or personal relationships that could have appeared to influence the work reported in this paper.

Data availability

Data will be made available on request.

Acknowledgments

We would like to thank Elinor Larsson for excellent technical assistance in flow cytometry analysis and *in vivo* experiments.

Appendix A. Supplementary data

Supplementary data to this article can be found online at https://doi.org/10.1016/j.cellimm.2024.104814.

References

[1] S. Sakaguchi, T. Yamaguchi, T. Nomura, M. Ono, Regulatory T cells and immune tolerance, Cell 133 (2008) 775–787.
[2] A. Facciabene, G.T. Motz, G. Coukos, T-regulatory cells: key players in tumor immune escape and angiogenesis, Cancer Res. 72 (2012) 2162–2171.
[3] H. Suzuki, M. Motegi, T. Akagi, Y. Hosokawa, M. Seto, API1-MALT1-MLT is involved in mucosa-associated lymphoid tissue lymphoma with t(11;18)(q21;q21), Blood 94 (1999) 3270–3271.
[4] J. Dierlamm, M. Baens, I. Wlodarska, M. Stefanova-Ouzounova, J.M. Hernandez, D. K. Hossfeld, et al., The apoptosis inhibitor gene API2 and a novel 18q gene, MLT, are recurrently rearranged in the t(11;18)(q21;q21) associated with mucosa-associated lymphoid tissue lymphomas, Blood 93 (1999) 3601–3609.
[5] V.N. Ngo, R.E. Davis, L. Lamy, X. Yu, H. Zhao, G. Lenz, et al., A loss-of-function RNA interference screen for molecular targets in cancer, Nature 441 (2006) 106–110.
[6] S. Hailfinger, G. Lenz, V. Ngo, A. Posvitz-Fejfar, F. Rebeaud, M. Guzzardi, et al., Essential role of MALT1 protease activity in activated B cell-like diffuse large B-cell lymphoma, PNAS 106 (2009) 19946–19951.
[7] F. Rebeaud, S. Hailfinger, A. Posevitz-Fejfar, M. Tapernoux, R. Moser, D. Rueda, et al., The proteolytic activity of the paracaspase MALT1 is key in T cell activation, Nat. Immunol. 9 (2008) 272–281.
[8] J. Ruland, G.S. Duncan, A. Wakeham, T.W. Mak, Differential requirement for Malt1 in T and B cell antigen receptor signaling, Immunity 19 (2003) 749–758.
[9] M. Thome, J. Tschopp, TCR-induced NF-kappaB activation: a crucial role for Carma1, Bcl10 and MALT1, Trends Immunol. 24 (2003) 419–424.
[10] J.W. Yu, S. Hoffman, A.M. Beal, A. Dykon, M.A. Ringenberg, A.C. Hughes, et al., MALT1 protease activity is required for innate and adaptive immune responses, PLoS One 10 (2015) e0127083.
[11] K. Martin, R. Touil, Y. Kolb, G. Cvijetic, K. Murakami, L. Israel, et al., Malt1 protease deficiency in mice disrupts immune homeostasis at environmental barriers and drives systemic T cell-mediated autoimmunity, J. Immunol. 203 (2019) 2791–2806.
[12] M. Jaworski, B.J. Marsland, J. Gehrig, W. Held, S. Favre, S.A. Luther, et al., Malt1 protease inactivation efficiently dampens immune responses but causes spontaneous autoimmunity, EMBO J. 33 (2014) 2765–2781.
[13] F. Bornancin, F. Renner, R. Touil, H. Sic, Y. Kolb, I. Touil-Allaoui, et al., Deficiency of MALT1 paracaspase activity results in unbalanced regulatory and effector T and B cell responses leading to multiorgan inflammation, J. Immunol. 194 (2015) 3723–3734.
[14] A. Gewies, O. Gorka, H. Bergmann, K. Pechloff, F. Petermann, K.M. Jeltsch, et al., Uncoupling Malt1 threshold function from paracaspase activity results in destructive autoimmune inflammation, Cell Rep. 9 (2014) 1292–1305.
[15] M. Baens, L. Bonsignore, R. Somers, C. Vanderheydt, S.D. Weeks, J. Gunnarsson, et al., MALT1 auto-proteolysis is essential for NF-κB-dependent gene transcription in activated lymphocytes, PLoS One 9 (2014) e103774.
[16] S. Ginster, M. Bardet, A. Unterreiner, C. Malinverni, F. Renner, S. Lam, et al., Two antagonistic MALT1 auto-cleavage mechanisms reveal a role for TRAF6 to unleash MALT1 activation, PLoS One 12 (2017) e0169026.
[17] B. Coornaert, M. Baens, K. Heyninck, T. Bekaert, M. Haegman, J. Staal, et al., T cell antigen receptor stimulation induces MALT1 paracaspase-mediated cleavage of the NF-kappaB inhibitor A20, Nat. Immunol. 9 (2008) 263–271.
[18] J. Staal, Y. Driege, T. Bekaert, A. Demeyer, D. Muyllaert, P. Van Damme, et al., T-cell receptor-induced JNK activation requires proteolytic inactivation of CYLD by MALT1, EMBO J. 30 (2011) 1742–1752.
[19] T. Klein, S.Y. Fung, F. Renner, M.A. Blank, A. Dufour, S. Kang, et al., The paracaspase MALT1 cleaves HOIL1 reducing linear ubiquitination by LUBAC to dampen lymphocyte NF-κB signalling, Nat. Commun. 6 (2015) 8777.
[20] L. Elton, I. Carpentier, J. Staal, Y. Driege, M. Haegman, R. Beyaert, MALT1 cleaves the E3 ubiquitin ligase HOIL-1 in activated T cells, generating a dominant negative inhibitor of LUBAC-induced NF-kappaB signaling, FEBS J. 283 (2016) 403–412.
[21] S.Y. Fung, H.Y. Lu, M. Sharma, A.A. Sharma, A. Saferali, A. Jia, et al., MALT1-dependent cleavage of HOIL1 modulates canonical NF-kappaB signaling and inflammatory responsiveness, Front. Immunol. 12 (2021) 749794.
[22] S. Hailfinger, H. Nogai, C. Pelzer, M. Jaworski, K. Cabalzar, J.E. Charton, et al., Malt1-dependent RelB cleavage promotes canonical NF-kappaB activation in lymphocytes and lymphoma cell lines, PNAS 108 (2011) 14596–14601.
[23] A. Brustle, D. Brenner, C.B. Knobbe-Thomsen, M. Cox, P.A. Lang, K.S. Lang, et al., MALT1 is an intrinsic regulator of regulatory T cells, Cell Death Differ. 24 (2017) 1214–1223.
[24] M. Rosenbaum, A. Gewies, K. Pechloff, C. Heuser, T. Engleitner, T. Gehring, et al., Bcl10-controlled Malt1 paracaspase activity is key for the immune suppressive function of regulatory T cells, Nat. Commun. 10 (2019) 2352.
[25] M. Baens, R. Stirparo, Y. Lampi, D. Verbeke, R. Vandepoel, J. Cools, et al., Malt1 self-cleavage is critical for regulatory T cell homeostasis and anti-tumor immunity in mice, Eur. J. Immunol. 48 (2018) 1728–1738.
[26] M. Di Pilato, E.Y. Kim, B.L. Cadilha, J.N. Prussmann, M.N. Nasrallah, D. Seruggia, et al., Targeting the CBM complex causes T(reg) cells to prime tumours for immune checkpoint therapy, Nature 570 (2019) 112–116.

[27] M. Di Pilato, Y. Gao, Y. Sun, A. Fu, C. Grass, T. Seeholzer, et al., Translational studies using the MALT1 inhibitor (S)-mepazine to induce treg fragility and potentiate immune checkpoint therapy in cancer, J. Immunother. Precis Oncol 6 (2023) 61–73.
[28] L. Cheng, N. Deng, N. Yang, X. Zhao, X. Lin, Malt1 protease is critical in maintaining function of regulatory T cells and may be a therapeutic target for antitumor immunity, J. Immunol. 202 (2019) 3008–3019.
[29] L. Fontan, C. Yang, V. Kabaleeswaran, L. Volpon, M.J. Osborne, E. Beltran, et al., MALT1 small molecule inhibitors specifically suppress ABC-DLBCL in vitro and in vivo, Cancer Cell 22 (2012) 812–824.
[30] L. Fontan, A. Melnick, Molecular pathways: targeting MALT1 paracaspase activity in lymphoma, Clin. Cancer Res. 19 (2013) 6662–6668.
[31] C. e. a. Pissot Soldermann. Novartis AG. Novel pyrazolo pyrimidine derivatives and their use as MALT1 inhibitors, PCT/IB2015/053975.
[32] J. Quancard, O. Simic, C. Pissot Soldermann, R. Aichholz, M. Blatter, M. Renatus, et al., Optimization of the in vivo potency of pyrazolopyrimidine MALT1 protease inhibitors by reducing metabolism and increasing potency in whole blood, J. Med. Chem. 63 (2020) 14594–14608.
[33] M. Bardet, A. Unterreiner, C. Malinverni, F. Lafossas, C. Vedrine, D. Boesch, et al., The T-cell fingerprint of MALT1 paracaspase revealed by selective inhibition, Immunol. Cell Biol. 96 (2018) 81–99.
[34] S. Biswas, A. Chalishazar, Y. Helou, J. DiSpirito, B. DeChristopher, D. Chatterjee, et al., Pharmacological inhibition of MALT1 ameliorates autoimmune pathogenesis and can be uncoupled from effects on regulatory T-cells, Front. Immunol. 13 (2022) 875320.
[35] E. Sato, S.H. Olson, J. Ahn, B. Bundy, H. Nishikawa, F. Qian, et al., Intraepithelial CD8+ tumor-infiltrating lymphocytes and a high CD8+/regulatory T cell ratio are associated with favorable prognosis in ovarian cancer, PNAS 102 (2005) 18538–18543.
[36] A. Tanaka, S. Sakaguchi, Targeting treg cells in cancer immunotherapy, Eur. J. Immunol. 49 (2019) 1140–1146.
[37] I. Hamp, T.J. O'Neill, O. Plettenburg, D. Krappmann, A patent review of MALT1 inhibitors (2013-present), Expert Opin. Ther. Pat. 31 (2021) 1079–1096.
[38] A. Loskog, C. Ninalga, G. Paul-Wetterberg, M. de la Torre, P.U. Malmstrom, T. H. Totterman, Human bladder carcinoma is dominated by T-regulatory cells and Th1 inhibitory cytokines, J. Urol. 177 (2007) 353–358.
[39] R. Murai, Y. Itoh, S. Kageyama, M. Nakayama, H. Ishigaki, K. Teramoto, et al., Prediction of intravesical recurrence of non-muscle-invasive bladder cancer by evaluation of intratumoral Foxp3+ T cells in the primary transurethral resection of bladder tumor specimens, PLoS One 13 (2018) e0204745.
[40] C. Mc Guire, L. Elton, P. Wieghofer, J. Staal, S. Voet, A. Demeyer *et al.* Pharmacological inhibition of MALT1 protease activity protects mice in a mouse model of multiple sclerosis. J. Neuroinflammation, 2014;11:124.
[41] K. Martin, U. Junker, E. Tritto, E. Sutter, T. Rubic-Schneider, H. Morgan, et al., Pharmacological inhibition of MALT1 protease leads to a progressive IPEX-like pathology, Front. Immunol. 11 (2020) 745.
[42] M. de la Rosa, S. Rutz, H. Dorninger, A. Scheffold, Interleukin-2 is essential for CD4+CD25+ regulatory T cell function, Eur. J. Immunol. 34 (2004) 2480–2488.
[43] S.M. Mangsbo, L.C. Sandin, K. Anger, A.J. Korman, A. Loskog, T.H. Totterman, Enhanced tumor eradication by combining CTLA-4 or PD-1 blockade with CpG therapy, J. Immunother. 33 (2010) 225–235.
[44] K.S. Peggs, S.A. Quezada, C.A. Chambers, A.J. Korman, J.P. Allison, Blockade of CTLA-4 on both effector and regulatory T cell compartments contributes to the antitumor activity of anti-CTLA-4 antibodies, J. Exp. Med. 206 (2009) 1717–1725.
[45] L. van Hooren, L.C. Sandin, I. Moskalev, P. Ellmark, A. Dimberg, P. Black, et al., Local checkpoint inhibition of CTLA-4 as a monotherapy or in combination with anti-PD1 prevents the growth of murine bladder cancer, Eur. J. Immunol. 47 (2017) 385–393.
[46] M. Nakaya, Y. Xiao, X. Zhou, J.H. Chang, M. Chang, X. Cheng, et al., Inflammatory T cell responses rely on amino acid transporter ASCT2 facilitation of glutamine uptake and mTORC1 kinase activation, Immunity 40 (2014) 692–705.
[47] K.M. Jeltsch, D. Hu, S. Brenner, J. Zoller, G.A. Heinz, D. Nagel, et al., Cleavage of roquin and regnase-1 by the paracaspase MALT1 releases their cooperatively repressed targets to promote T(H)17 differentiation, Nat. Immunol. 15 (2014) 1079–1089.
[48] D. Shevyrev, V. Tereshchenko, Treg heterogeneity, function, and homeostasis, Front. Immunol. 10 (2019) 3100.
[49] L. Wang, D.L. Simons, X. Lu, T.Y. Tu, S. Solomon, R. Wang, et al., Connecting blood and intratumoral T(reg) cell activity in predicting future relapse in breast cancer, Nat. Immunol. 20 (2019) 1220–1230.